NASA TECHNICAL NOTE

NASA TN D-5555

NASA TN D-5555

FLUTTER DESIGN OF STIFFENED-SKIN PANELS FOR HYPERSONIC AIRCRAFT

by Herman L. Bohon, Melvin S. Anderson, and Walter L. Heard, Jr.

Langley Research Center
Langley Station, Hampton, Va.

NATIONAL AERONAUTICS AND SPACE ADMINISTRATION • WASHINGTON, D. C. • DECEMBER 1969

1. Report No. NASA TN D-5555	2. Government Accession No.	3. Recipient's Catalog No.
4. Title and Subtitle FLUTTER DESIGN OF STIFFENED-SKIN PANELS FOR HYPERSONIC AIRCRAFT		5. Report Date December 1969 6. Performing Organization Code
7. Author(s) Herman L. Bohon, Melvin S. Anderson, and Walter L. Heard, Jr.		8. Performing Organization Report No. L-6106 10. Work Unit No. 126-14-14-06-23
9. Performing Organization Name and Address NASA Langley Research Center Hampton, Va. 23365		11. Contract or Grant No. 13. Type of Report and Period Covered Technical Note
12. Sponsoring Agency Name and Address National Aeronautics and Space Administration Washington, D.C. 20546		14. Sponsoring Agency Code

15. Supplementary Notes

16. Abstract

Factors which control the flutter design for exterior skin panels of hypersonic vehicles are reviewed. From a typical trajectory the most critical flight regime is identified in the supersonic range. Because past studies have shown that support flexibility can seriously reduce the flutter margin of panels such as those proposed for hypersonic vehicles, conservative design curves for such panels with flexible supports are presented. Means of greatly improving flutter margins by the addition of torsional restraint at the panel edges are also indicated.

17. Key Words Suggested by Author(s)	18. Distribution Statement		
Flutter Flutter of stiffened panels Hypersonic flutter design Corrugation-stiffened panels Flutter design boundaries	Unclassified - Unlimited		
19. Security Classif. (of this report) Unclassified	20. Security Classif. (of this page) Unclassified	21. No. of Pages 26	22. Price* $3.00

*For sale by the Clearinghouse for Federal Scientific and Technical Information Springfield, Virginia 22151

FLUTTER DESIGN OF STIFFENED-SKIN PANELS FOR HYPERSONIC AIRCRAFT

By Herman L. Bohon, Melvin S. Anderson,
and Walter L. Heard, Jr.
Langley Research Center

SUMMARY

Factors which control the flutter design for exterior skin panels of hypersonic vehicles are reviewed. From a typical trajectory the most critical flight regime is identified in the supersonic range. Because past studies have shown that support flexibility can seriously reduce the flutter margin of panels such as those proposed for hypersonic vehicles, conservative design curves for such panels with flexible supports are presented. Means of greatly improving flutter margins by the addition of torsional restraint at the panel edges are also indicated.

INTRODUCTION

External skin panels of hypersonic aircraft will consist of various stiffened panels that may be subject to flutter in the supersonic and hypersonic operating range. Studies indicate that these panels will be of more complicated construction than current practice in order to withstand the hostile environment with minimum mass. Although a wealth of experimental data on the flutter of flat panels has been accumulated over the past few years (ref. 1), only a small portion of the data was obtained from stiffened-skin panels. Further, only within the past 5 years have flutter data been generated at Mach numbers higher than Mach 5 (ref. 2), and nearly all these data have been obtained from isotropic panels. Nevertheless, data on isotropic panels suggest that panel flutter boundaries based on supersonic aerodynamic theory can be extended into the hypersonic range. Further, consideration of the flight envelope for proposed hypersonic cruise vehicles indicates the most critical portion of the flight from a flutter standpoint is in the supersonic-speed range. It is in this speed range that most flutter data on orthotropic panels have been obtained. Thus, the use of these data and recent theory derived for the supersonic-speed range permit the assessment of panel flutter design for hypersonic vehicles. In the present paper the available experimental and theoretical information is used to identify the critical flutter problems and a simplified approach for hypersonic vehicle panel design is given.

SYMBOLS

The units used for the physical quantities in this paper are given both in the U.S. Customary Units and in the International System of Units (SI). Factors relating the two systems are given in the appendix for the units used in the present investigation.

$\overline{A}_x, \overline{A}_y$ stiffness-geometry parameter for airflow in x- and y-direction, respectively

a,b panel dimension in x- and y-direction, respectively

$C = \frac{D_{12}}{D_1 D_2}$

D panel bending stiffness

D_1, D_2 panel bending stiffness in x- and y-direction, respectively (see fig. 4)

D_{12} panel twisting stiffness

k_D, k_R, k_T deflectional, rotational, and torsional spring constant, respectively

$K_D = \frac{k_D b^3}{\pi^3 D_2}$

$K_R = \frac{k_R b}{\pi D_2}$

$K_T = \frac{k_T b}{\pi D_2}$

M_l local Mach number

M_∞ free-stream Mach number

q dynamic pressure

q_{cr} critical dynamic pressure for flutter

x,y coordinates (see fig. 4)

ω circular frequency

$\omega_r = \frac{\pi^2}{a^2}\sqrt{\frac{D_1}{\gamma}}$

α angle of attack

λ_{cr} critical flutter parameter with airflow in y-direction, $\frac{2qb^3}{D_2\sqrt{M_l^2 - 1}}$

λ^*_{cr} critical flutter parameter with airflow in x-direction, $\frac{2qb^3}{D_1\sqrt{M_l^2 - 1}}\left(\frac{D_1}{D_{12}}\right)^{3/2}$

γ mass per unit area

FLUTTER DESIGN CONSIDERATIONS FOR PANELS OF HYPERSONIC VEHICLES

External skin panels of hypersonic vehicles will be exposed to a wide range of dynamic pressure, Mach number, and temperature. The impact of some of these parameters on panel flutter design is discussed in the following sections.

Effects of Mach Number

Experimental flutter data generated from flat isotropic panels at high Mach numbers (see ref. 2) have shown reasonable agreement with trends predicted by using small-deflection plate theory with quasi-static aerodynamics, as illustrated in figure 1, where the parameter $q/D\sqrt{M_l^2 - 1}$ is plotted as a function of local Mach number. The solid line is the flutter boundary, which separates the "flutter" region (above the line) from the "no flutter" region (below the line). This boundary, based on quasi-static aerodynamics, is constant with respect to Mach number and extends into the hypersonic range. The symbols represent experimental flutter data from reference 2, obtained from isotropic panels over the range of Mach numbers from 2 to 6. The agreement (considered good for panel flutter) of the experimental data with theory over the entire Mach number range in figure 1 suggests that the flutter boundary may be applied further in the hypersonic range than shown in figure 1 with reasonable success. The fact that the flutter boundary is not dependent on Mach number also suggests that panels on a hypersonic vehicle will be most susceptible to flutter wherever the flight path produces the maximum value of $q\sqrt{M_l^2 - 1}$ (if the panel bending stiffness D is assumed to be constant). Thus, trajectories for the hypersonic vehicle need to be examined to determine where the maximum value occurs.

Figure 2 shows the variation of the parameter $q/\sqrt{M_l^2 - 1}$ with free-stream Mach number for the wing lower surface of a hypersonic cruise vehicle in a typical ascent trajectory. In the parameter, the dynamic pressure and the Mach number are local conditions. The lower curve represents the local flow conditions over a flat surface at zero angle of attack, whereas the upper curve corresponds to flow conditions on the wing lower surface at angle of attack of 3^o during the early part of the flight and to an angle of attack of 5^o during the final climb at constant dynamic pressure. The point where a panel is most susceptible to flutter is at the maximum value of $q/\sqrt{M_l^2 - 1}$, which occurs on this flight path in the vicinity of Mach 3. Several other advanced vehicle trajectories, examined in reference 3, have led to the same conclusion – that the supersonic range is most critical from a flutter standpoint.

The results of figure 2 would be modified slightly if the effect of elevated temperatures on the panel bending stiffness D is considered. However, since the design condition for flutter is in the supersonic range where temperatures are generally low relative to material capability, the effect of variable D would be small.

No mention has been made of the transonic range where, as is well known from experimental data, reductions in the critical value of $q/\sqrt{M_l^2 - 1}$ occur. (See refs. 4, 5, and 6.) Note, however, from figure 2 that the value of $q/\sqrt{M_l^2 - 1}$ encountered on the flight path also decreases in the transonic range; this reduction is generally greater than that obtained experimentally for flutter. Consequently, flutter in the transonic range is not pursued further in this paper.

Effects of Panel Construction and Boundary Conditions

Most experimental data available on stiffened panels suitable for a hypersonic vehicle have been obtained in the supersonic range where problem areas having special significance with regard to panel flutter design have been well delineated. Since supersonic flutter analyses and experiments are pertinent to the hypersonic range, the effects of these problems on hypersonic panel design can be determined.

Panel configurations appropriate for use on the hypersonic vehicle include waffle-grid, honeycomb core sandwich, or corrugation-stiffened panels with either chordwise or spanwise orientation. One of the primary design problems associated with such panels is the method of attachment to the supports. The sensitivity of panel flutter to support conditions is illustrated in figure 3, which shows two typical methods of attaching corrugation-stiffened panels at the ends of the corrugations. The panels which were identical except for support conditions were tested at Mach 3 with the corrugations alined normal to the airflow; thus, the weaker of the panel bending stiffnesses D_1 is in the airflow direction. (Test details are reported in ref. 7.) In one test the corrugations at the edges were

attached to an angle clip; the panel fluttered at a dynamic pressure q of 3400 psf (163 kN/m^2). The same panel, when tested with the clip removed (that is, with the corrugations unsupported), fluttered at a dynamic pressure q of 540 psf (25.8 kN/m^2). Thus, the flutter margin was reduced by more than a factor of 6 simply by a relaxation of the stiffness of the supports at the ends of the corrugations. In order to determine analytically the flutter mechanisms involved in these and other similar tests, the problem has been formulated, in the next section, to account for arbitrary deflectional stiffness at the supports.

ANALYTICAL RESULTS FOR ORTHOTROPIC PANELS

An orthotropic panel and the coordinate system are shown in figure 4. The edges at $x = 0$ and $x = a$ are simply supported. The edges at $y = \pm b/2$ are supported by deflectional springs with a spring constant k_D per unit length. These edge conditions may account for flexibility of the supports as well as for local deformations of the cross section at the support. The panel has been analyzed for airflow (at Mach number M_l) parallel either to the x-direction or the y-direction; the lateral loading due to the air forces is given by the two-dimensional static approximation. For details of the analytical development, see reference 8. Numerical results obtained are applicable to any combination of bending and twisting stiffnesses and panel geometry, but the main part of the discussion herein applies to orthotropic panels for which D_1 is much less than D_{12}, which is, in turn, less than D_2.

Spring Supports on Leading and Trailing Edges

When the airflow is parallel to the y-direction (direction of strong flexural stiffness), the leading and trailing edges are supported by deflectional springs. Results, obtained from a closed-form solution for zero midplane stress, are shown in figure 5 on a plot of λ_{cr}, the dynamic pressure parameter at flutter, as a function of stiffness-geometry parameter $-\overline{A}_y$ for various values of nondimensional spring constant K_D. It should be noted that the panel dimension b is in the airflow direction. Flutter boundaries are shown for finite values of spring constant K_D of 1, 5, and 10. The upper curve for $K_D = \infty$ is the flutter boundary for the panel with all edges simply supported. Values of K_D as low as 1 are not unreasonable, and the figure shows that support flexibility can reduce the flutter dynamic pressure q by as much as a factor of 10 from the simple-support value. At low values of $-\overline{A}_y$ (panels with corrugations alined with the airstream), the curves become horizontal; hence, the flutter boundaries become independent of the panel width a and of the support conditions along the streamwise edges. In fact, the panel behaves as if it were infinitely long in the weak bending direction (that is, the x-direction).

Spring Supports on Streamwise Edges

When the airflow is parallel to the x-direction (that is, normal to the direction of corrugations), the spring supports are at the streamwise edges. A closed-form solution could not be found for this support condition; instead, a Galerkin solution which used up to 50 natural panel vibration modes to assure convergence was obtained. The analysis is presented in reference 8, and some numerical flutter results are shown in figure 6.

The parameters in figure 6 are slightly modified compared with those of figure 5 as a result of the different direction of airflow. The cube root of λ_{cr}^{*} is plotted as a function of $-\overline{A}_x$ for various values of K_D. However, for this analysis the results are also a function of the parameter C, which is a ratio of panel stiffnesses shown in the figure. A representative value of $C = 7$ was used for these calculations. The curves for finite values of K_D are bounded above by the limiting curve for $K_D = \infty$ (that is, for simply supported edges), which is obtained from an exact solution, and below by the limiting curve for $K_D = 0$ (that is, for free edges), which is also obtained from an exact solution. The cusps in the curves are caused by changes in critical modes which coalesce for flutter. The numerals in the regions separated by the dashed curves indicate the modes that coalesce to give the critical flutter boundary.

For corrugation-stiffened panels, the ratio D_{12}/D_1 is very large; therefore, the region of primary interest is the far right-hand section of figure 6. The results show that flexible supports may cause large reductions in λ_{cr}^{*}. In this region, the flutter boundaries become horizontal and the flutter dynamic pressure q becomes independent of the panel length a; thus, flutter results are independent of details of the boundary conditions at the leading and trailing edges.

Effect of Orientation of Corrugations

The effect of orientation of the corrugations with respect to the airstream is shown in figure 7 where a direct comparison is made between the results for flow parallel to and the results for flow perpendicular to the orientation of the corrugations. The comparison is made for a value of the ratio a/b equal 1. The dashed curves are from the exact analysis made with the corrugations oriented parallel to the airstream; the solid curves are from the modal analysis made with the corrugations oriented normal to the airstream. As noted previously, the modal results are functions of the stiffness parameter C; curves are shown only for $C = 7$. For orthotropic panels D_{12}/D_2 is small, and the results show a pronounced adverse effect of weak supports on the streamwise edges. Additional effects of panel orientation can be obtained from reference 9 where flutter boundaries for $K_D = \infty$ are presented for arbitrary angles of orientation and for several combinations of panel stiffnesses.

DESIGN BOUNDARIES

As indicated in the discussion of figures 5 and 6, panels of interest for hypersonic vehicles generally fall in the regions where the flutter boundaries become horizontal. These regions of minimum values may provide good, and often conservative, estimates of the flutter parameter for orthotropic panels and should be very useful for design purposes. The plot of such minimum values of critical flutter parameter is shown in figures 8 and 9 where λ_{cr} and λ^*_{cr}, respectively, are plotted as a function of K_D over the range from $K_D = 0$ (free edges) to $K_D = \infty$ (simply supported edges). A family of curves is shown in figure 9 for several values of the stiffness parameter C. The application of these curves by the design engineer requires a knowledge of the panel stiffnesses and geometry and a reliable estimate of the deflectional stiffness at the supports. Deflectional stiffness may be obtained experimentally from a vibration survey of the panel.

To date, no experimental flutter data have been obtained on orthotropic panels oriented with the maximum flexural stiffness in the airstream direction to verify or dispute the trends shown in figure 8. On the other hand, all experimental flutter data obtained to date on orthotropic panels have been with the maximum flexural stiffness normal to the airstream, as represented by the theoretical model for the curves in figure 9. A correlation of data from several experimental investigations with the present theory has been made and the results are shown in figure 10. The solid curves are repeated from figure 9 for $C = 7$ and $C = 20$. The experimental data represented by the symbols (taken from refs. 7, 10, 11, and 12) were obtained from corrugation-stiffened panels which exhibited flutter at Mach numbers from 1.2 to 3. The panels have a wide variety of edge-support conditions ranging from very weak supports, with the corrugations unsupported, to the attachment of the corrugations to a rigid substructure. Deflectional stiffnesses at the supports were not measured and were difficult to define. However, an estimate of the stiffness was made for the flexibility of the corrugations at the supports as well as the flexibility of the attachments. Details of deflectional stiffness calculations are presented in reference 12.

The diamond symbols in figure 10 are for values of C between 5.5 and 7 and with the exception of two test points, all lie in the flutter region above the curve for $C = 7$. The square symbols represent panels with intermediate values of C between 9 and 15, and the circular symbols represent panels with high values of C between 19 and 24. The data are seen to verify the trends of the theoretical curves and illustrate the fact that corrugation-stiffened panels tested to date have fluttered at dynamic pressures far less than the value provided by the conditions for all edges simply supported. Some of the data appearing in figure 10, along with data on isotropic panels have been used to generate empirical flutter envelopes in an effort to represent the lower limit of test data over a wide range of proportions. (See, for example, ref. 13.) No differentiation was made

between data for corrugation-stiffened panels (which show the large disparity from theory for simple support boundary conditions) and isotropic panels (which compare well with theory for simple support boundary conditions). It can be seen that such a flutter boundary would be overly conservative for any panel that had appreciable support stiffness. However, proper account of support flexibility results in reasonable agreement between theory and experiment.

DESIGN RECOMMENDATIONS

For the purpose of design of stiffened panels for flutter-free operations on the hypersonic vehicle, limiting flutter boundaries have been presented for both spanwise and streamwise orientation of maximum-stiffness corrugations. (See figs. 8 and 9.) Since these conservative boundaries show that support flexibility results in a rapid reduction in λ_{cr} and since some flexibility is inherent in the fabrication of complex stiffened structures, some degradation of the flutter boundary must be anticipated.

Recently, a method of support attachment has become apparent that may provide a sizable increase in λ_{cr} in the presence of support deflectional flexibility. This method involves the addition of a local torsional stiffness along the boundaries normal to the maximum-stiffness corrugations. For example, a corrugated doubler strap along the ends of corrugations provides considerable torsional stiffness at the boundary. The effect of torsional stiffness has been determined by an extension of the analysis of corrugation-stiffened panels presented in reference 8. A sample calculation is shown in figure 11 where λ_{cr}^{*} is plotted as a function of K_T for $K_D = 10$. For this calculation $a/b = 1$, $C = 7$, and $-\overline{A}_x = 100$. For $K_T = 0$, the value of λ_{cr}^{*} is the same as a point on the curve $K_D = 10$ from figure 6. As K_T increases, λ_{cr}^{*} is seen to increase and the curve for $K_D = 10$ eventually becomes asymptotic to the curve for $K_D = \infty$ (that is, for all edges simply supported). Thus, the addition of torsional boundary stiffness can compensate for lack of deflectional stiffness.

The effect of K_T on flutter has been verified to a degree by a recent experimental investigation conducted on corrugation-stiffened panels in the Langley 9- by 6-foot thermal structures tunnel at Mach 3. The panels were constructed with corrugated doublers welded to the panel corrugations at the edges. (See fig. 12(a).) These corrugated doublers provided torsional spring stiffness K_T; they were 0.60 inch (15.2 cm) wide and three times the thickness of the corrugated material. The panels were attached at the ends of each of the corrugations to carefully machined cantilevered beams (fig. 12(b)) in order to facilitate easy calculation of deflectional stiffness K_D and rotational stiffness K_R. The numerical value of K_T was obtained from measured natural frequencies shown in figure 13. The circular symbols are the measured frequencies corresponding to one

half-wave in the direction of the corrugations and to the first seven half-waves in the weak bending direction. The dashed curve gives the theoretical frequencies for the calculated values, $K_D = 0.64$ and $K_R = 0.15$, for $K_T = 0$. The solid curve yields theoretical frequencies for the same values of K_D and K_R, but for $K_T = 1.2$ and provides a realistic correlation of the measured frequencies, as can be seen from figure 13.

The panel with torsionally stiffened edges was tested at Mach 3, and the flutter data obtained is compared in figure 14 with the theoretical boundaries from figure 10. The experimental data obtained from the torsionally stiffened panel is shown by the bar symbol at $K_D = 0.64$. The panel was tested in the presence of aerodynamic heating and the height of the bar represents the range of flutter dynamic pressure as the result of thermal stress. The limited amount of data prevented definition of the experimental value of λ^*_{cr} for the unstressed panel. The theoretical prediction of λ^*_{cr} (shown by the cross) is for zero stress and $K_T = 1.2$. If experimental data had been obtained at zero stress, the comparison would be much improved. The significant fact is, however, that in the absence of a doubler strap along the corrugated edges (that is, for $K_T = 0$), the panel would probably flutter at a value of λ^*_{cr} slightly above the theoretical curve for $C = 7$ (the value of C of the panel tested is 6.1) at $K_D = 0.64$. The inclusion of the doubler may have increased λ^*_{cr} by as much as a factor of 30. Thus, it appears that a simple doubler strap at the corrugated edges or other methods of attachment which provide local torsional rigidity for the stiffening elements may result in large increases in flutter margin and improved efficiency in panel design.

CONCLUDING REMARKS

Existing flutter analyses and experimental data obtained in the supersonic Mach number range can be applied to the design of panels for the hypersonic speed range with reasonable success. Examination of a hypersonic-vehicle flight trajectory indicates that the most critical portion from a flutter standpoint is probably in the supersonic speed range.

Experimental studies in the supersonic speed range have shown that panels proposed for hypersonic vehicles flutter at dynamic pressures much less than anticipated based on classical flutter theory for panels with simply supported edges. This loss in flutter margin is attributed to deflectional support flexibility which is inherent in the usual fabrication of stiffened structures. Simple design curves are presented for such orthotropic panels and have been corroborated by the correlation of a large quantity of experimental data on corrugation-stiffened panels covering a wide range of test conditions and support conditions. Finally, it is demonstrated experimentally and analytically that even in the

presence of deflectional support flexibility, a large improvement in flutter margin can be realized by the addition of torsional restraint at the supports.

Langley Research Center,
National Aeronautics and Space Administration,
Langley Station, Hampton, Va., October 9, 1969.

APPENDIX

CONVERSION OF U.S. CUSTOMARY UNITS TO SI UNITS

The International System of Units (SI) was adopted by the Eleventh General Conference on Weights and Measures, Paris, October 1960, in Resolution No. 12 (ref. 14). Conversion factors for the units used herein are given in the following table:

Physical quantity	U.S. Customary Unit	Conversion factor (*)	SI Unit
Length	in.	0.0254	meters (m)
Stiffness	lbf-in.	0.113	newton-meter (N-m)
Pressure	lbf/ft^2	47.88	newtons/$meter^2$ (N/m^2)

*Multiply value given in U.S. Customary Unit by conversion factor to obtain equivalent value in SI Unit.

Prefixes to indicate multiples of units are as follows:

Prefix	Multiple
kilo (k)	10^3

REFERENCES

1. Johns, D. J.: A Survey on Panel Flutter. Presented to the Structures and Materials Panel of AGARD (Nancy, France), Nov. 1965.

2. Ketter, D. J.; and Voss, H. M.: Panel Flutter Analyses and Experiments in the Mach Number Range of 5.0 to 10.0. FDL-TDR-64-6, U.S. Air Force, Mar. 1964.

3. Langley, Bobby L.: A Study of Panel Thickness Required To Prevent Flutter in Advanced Performance Vehicles. 11th Annual Air Force Science and Engineering Symposium, U.S. Air Force, Oct. 1964.

4. Dixon, Sidney C.: Comparison of Panel Flutter Results From Approximate Aerodynamic Theory With Results From Exact Inviscid Theory and Experiment. NASA TN D-3649, 1966.

5. Cunningham, H. J.: Flutter Analysis of Flat Rectangular Panels Based on Three-Dimensional Supersonic Potential Flow. AIAA J., vol. 1, no. 8, Aug. 1963, pp. 1795-1801.

6. Dowell, E. H.; and Voss, H. M.: Experimental and Theoretical Panel Flutter Studies in the Mach Number Range 1.0 to 5.0. ASD-TDR-63-449, U.S. Air Force, Dec. 1963.

7. Weidman, Deene J.: Experimental Flutter Results for Corrugation-Stiffened and Unstiffened Panels. NASA TN D-3301, 1966.

8. Bohon, Herman L.; and Anderson, Melvin S.: Role of Boundary Conditions on Flutter of Orthotropic Panels. AIAA J., vol. 4, no. 7, July 1966, pp. 1241-1248.

9. Gaspers, Peter A., Jr.; and Redd, Bass: A Theoretical Analysis of the Flutter of Orthotropic Panels Exposed to a High Supersonic Stream of Arbitrary Direction. NASA TN D-3551, 1966.

10. Bohon, Herman L.: Experimental Flutter Results for Corrugation-Stiffened Panels at a Mach Number of 3. NASA TN D-2293, 1964.

11. Pride, Richard A.; Royster, Dick M.; and Helms, Bobbie F.: Design, Tests, and Analysis of a Hot Structure for Lifting Reentry Vehicles. NASA TN D-2186, 1964.

12. Bohon, Herman L.: Flutter of Corrugation-Stiffened Panels at Mach 3 and Comparison With Theory. NASA TN D-4321, 1968.

13. Kordes, Eldon E.; Tuovila, Weimer J.; and Guy, Lawrence D.: Flutter Research on Skin Panels. NASA TN D-451, 1960.

14. Comm. on Metric Pract.: ASTM Metric Practice Guide. NBS Handbook 102, U.S. Dep. Com., Mar. 10, 1967.

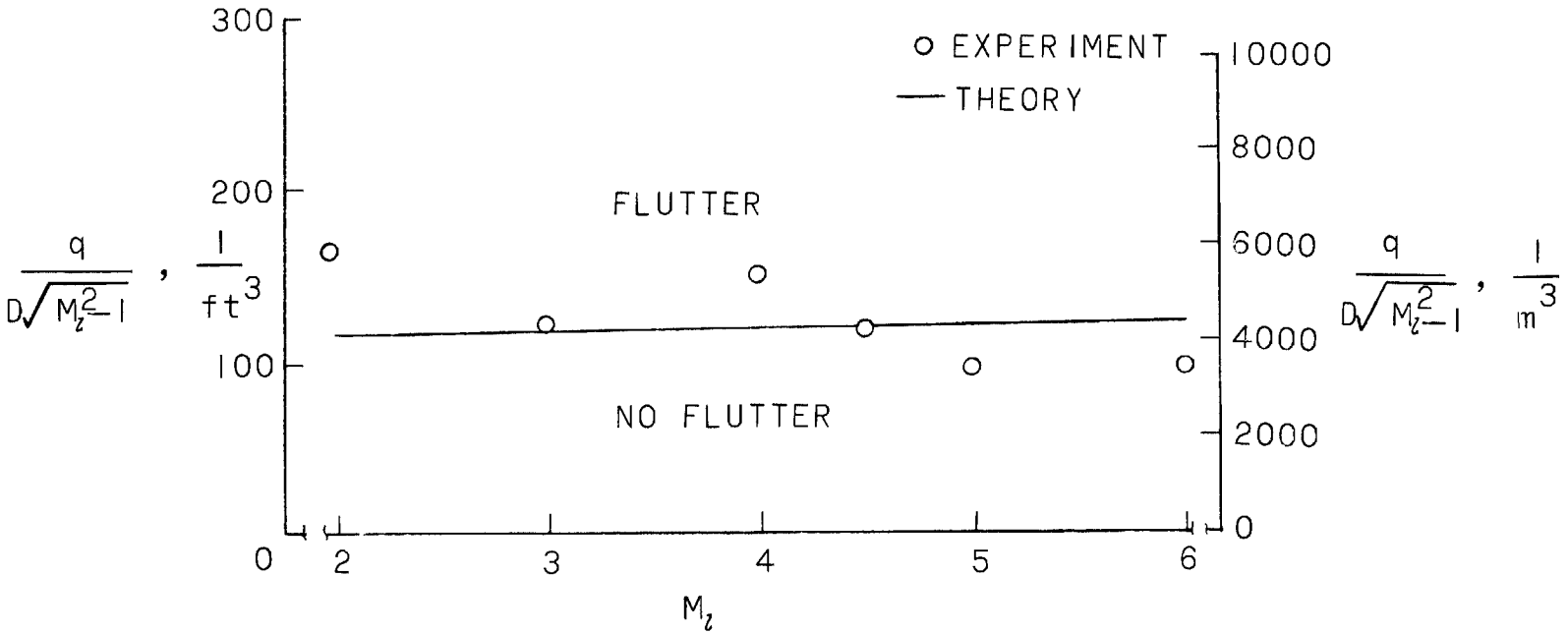

Figure 1.- Comparison of experiment and theory for the flutter boundary of clamped isotropic panels at various Mach numbers.

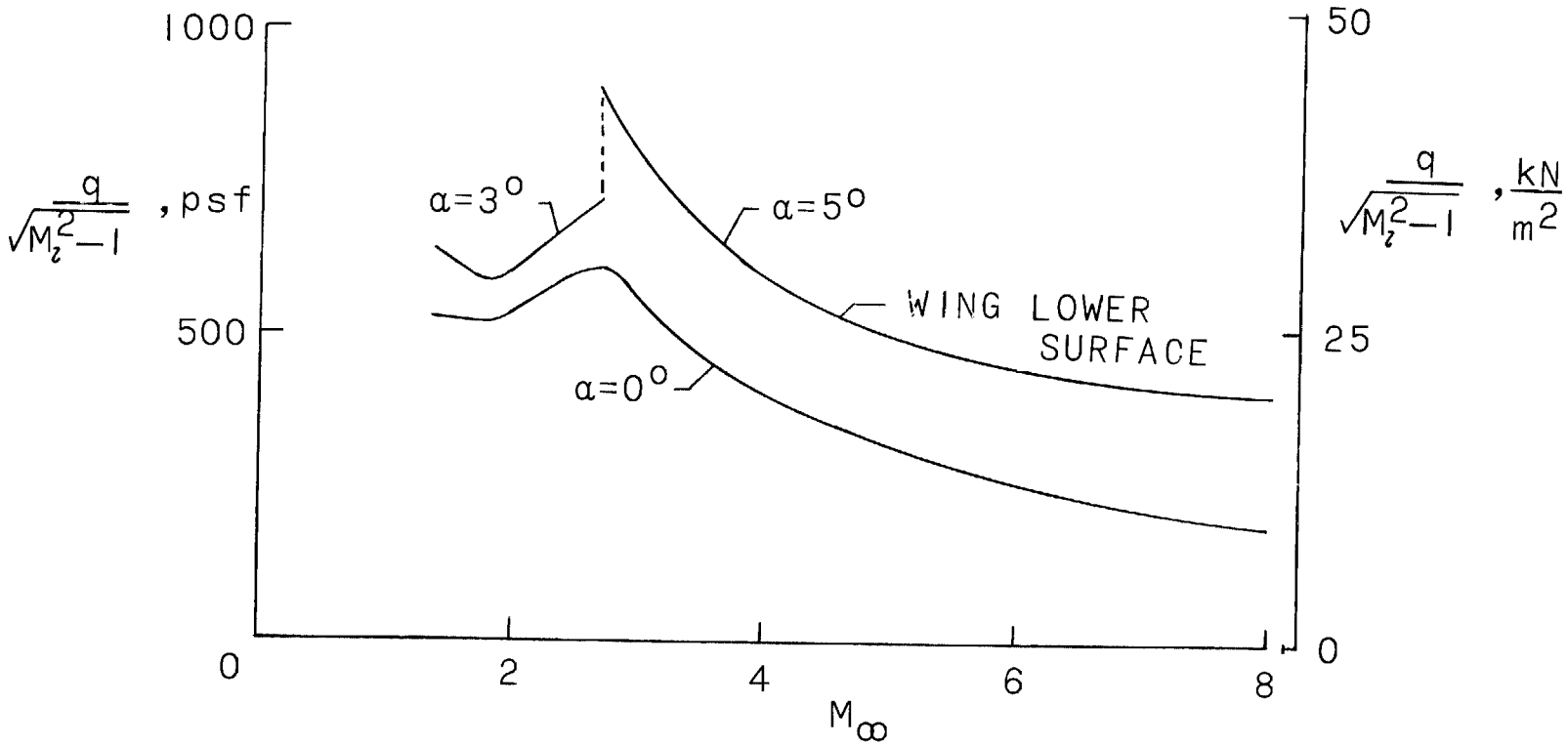

Figure 2.- Variation of flutter parameter on ascent trajectory for Mach 8 cruise vehicle.

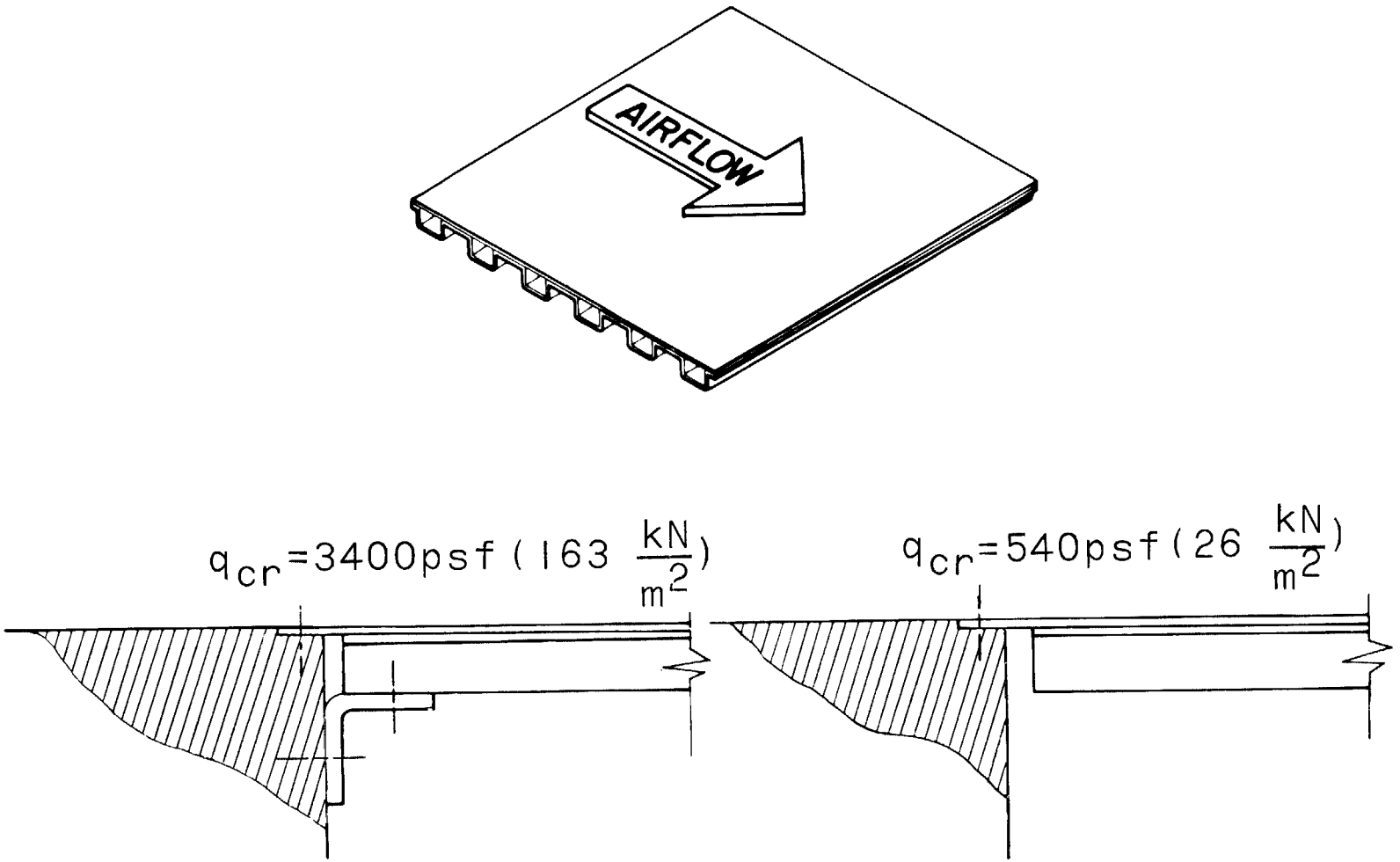

Figure 3.- Effect of edge-support conditions on panel flutter at Mach 3.

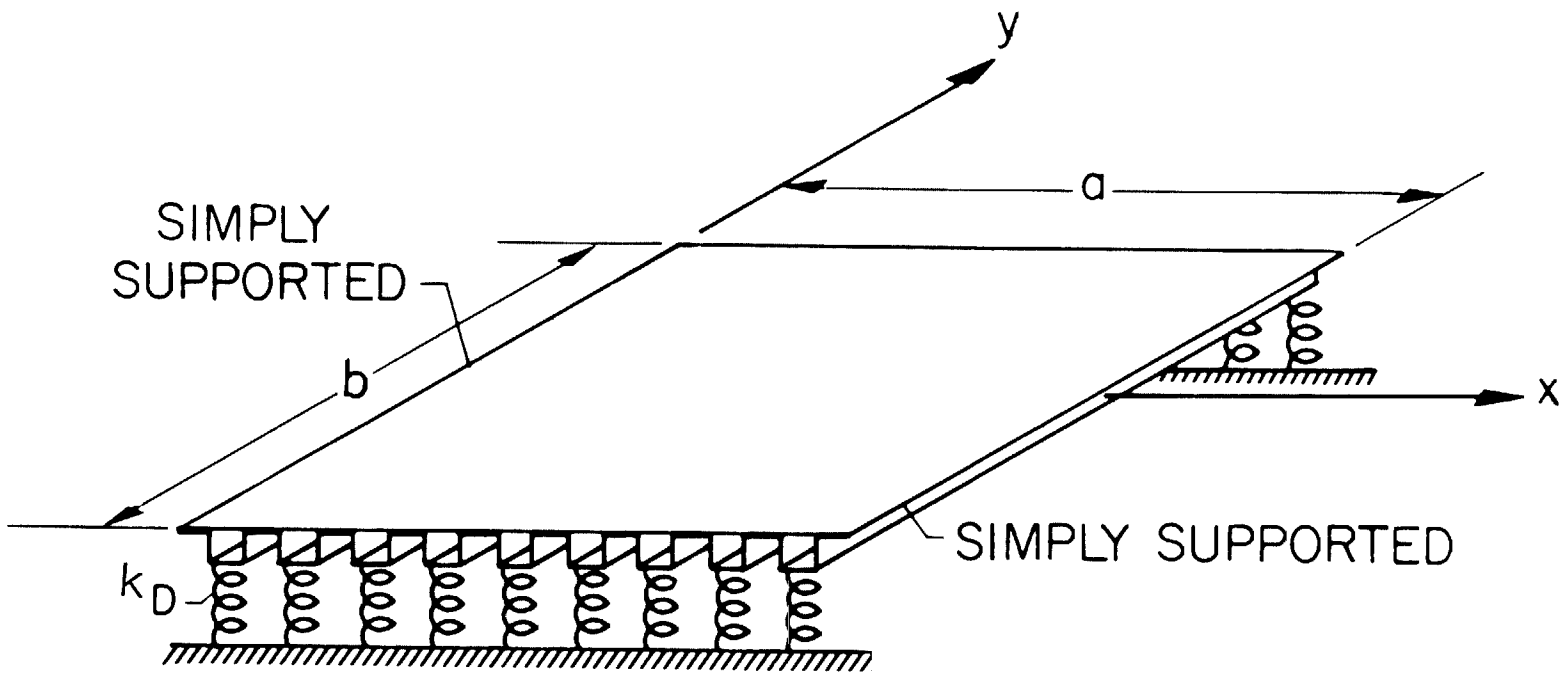

Figure 4.- Orthotropic panel and coordinate system.

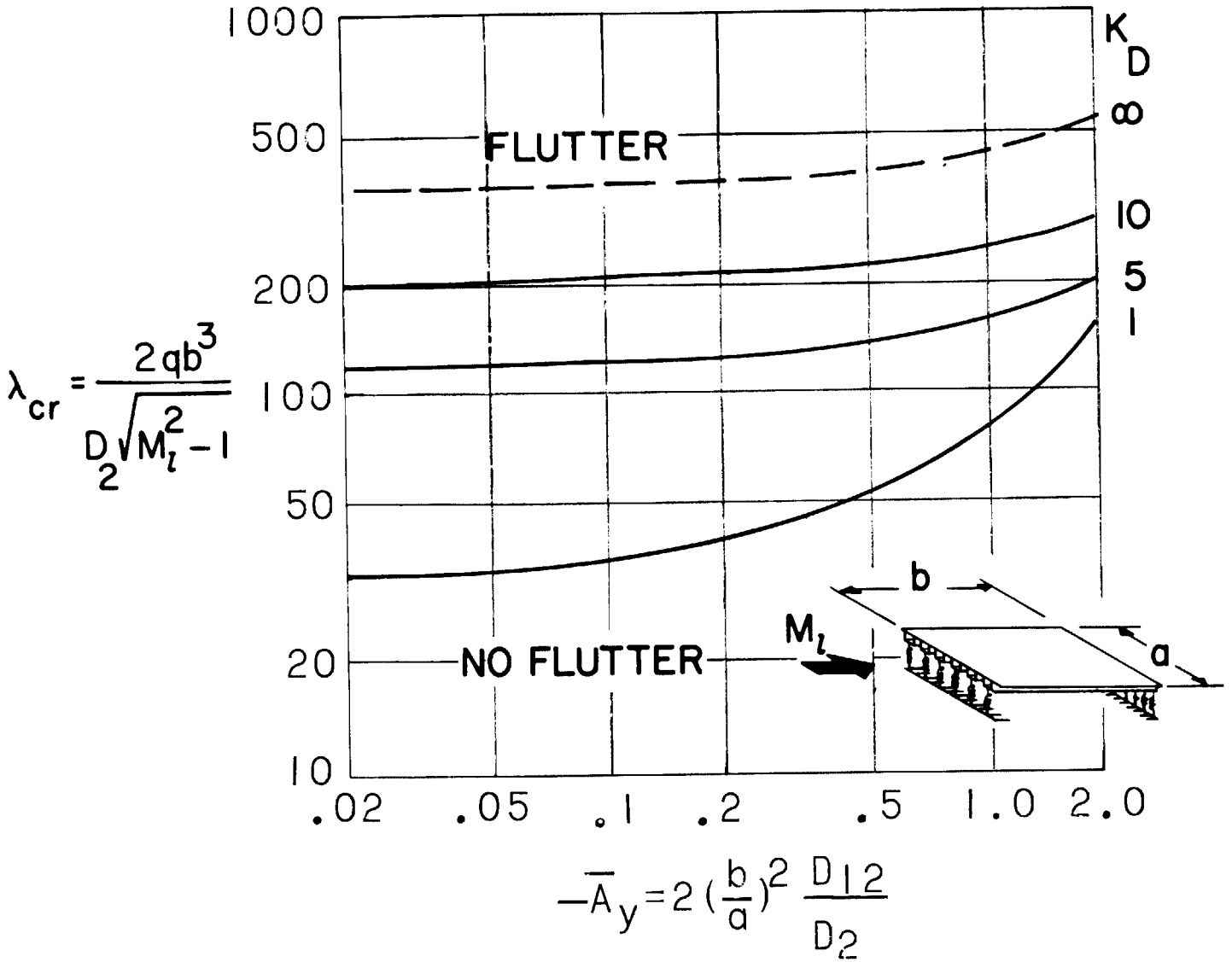

Figure 5.- Flutter boundary for flexible supports for flow in strong direction. (Exact solution.)

$$\left(\lambda^{*}_{cr}\right)^{1/3} = \left(\frac{2qb^{3}}{D_1\sqrt{M_l^{2}-1}}\right)^{1/3}\sqrt{\frac{D_1}{D_{12}}}$$

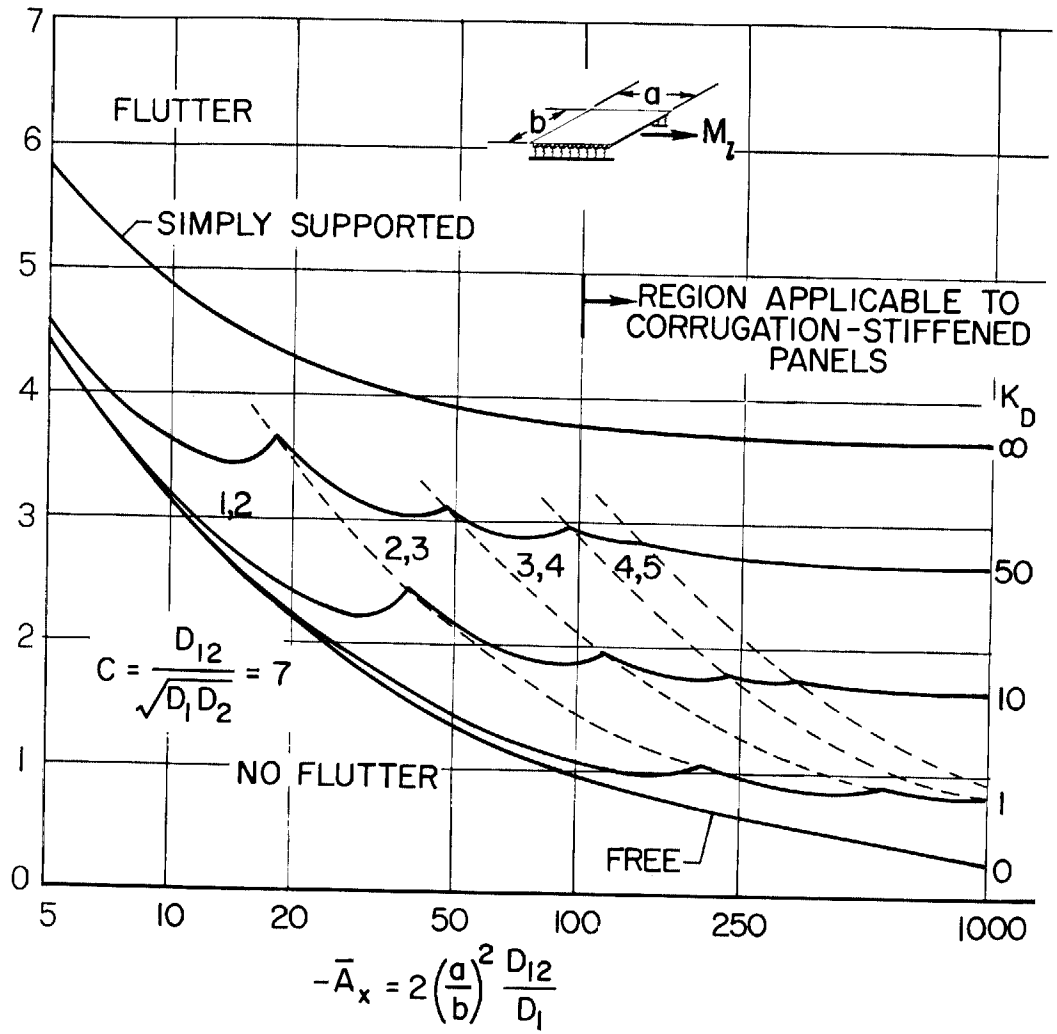

Figure 6.- Flutter boundary for flexible supports for flow in weak direction. (Modal solution.) Numbers on curves designate modes.

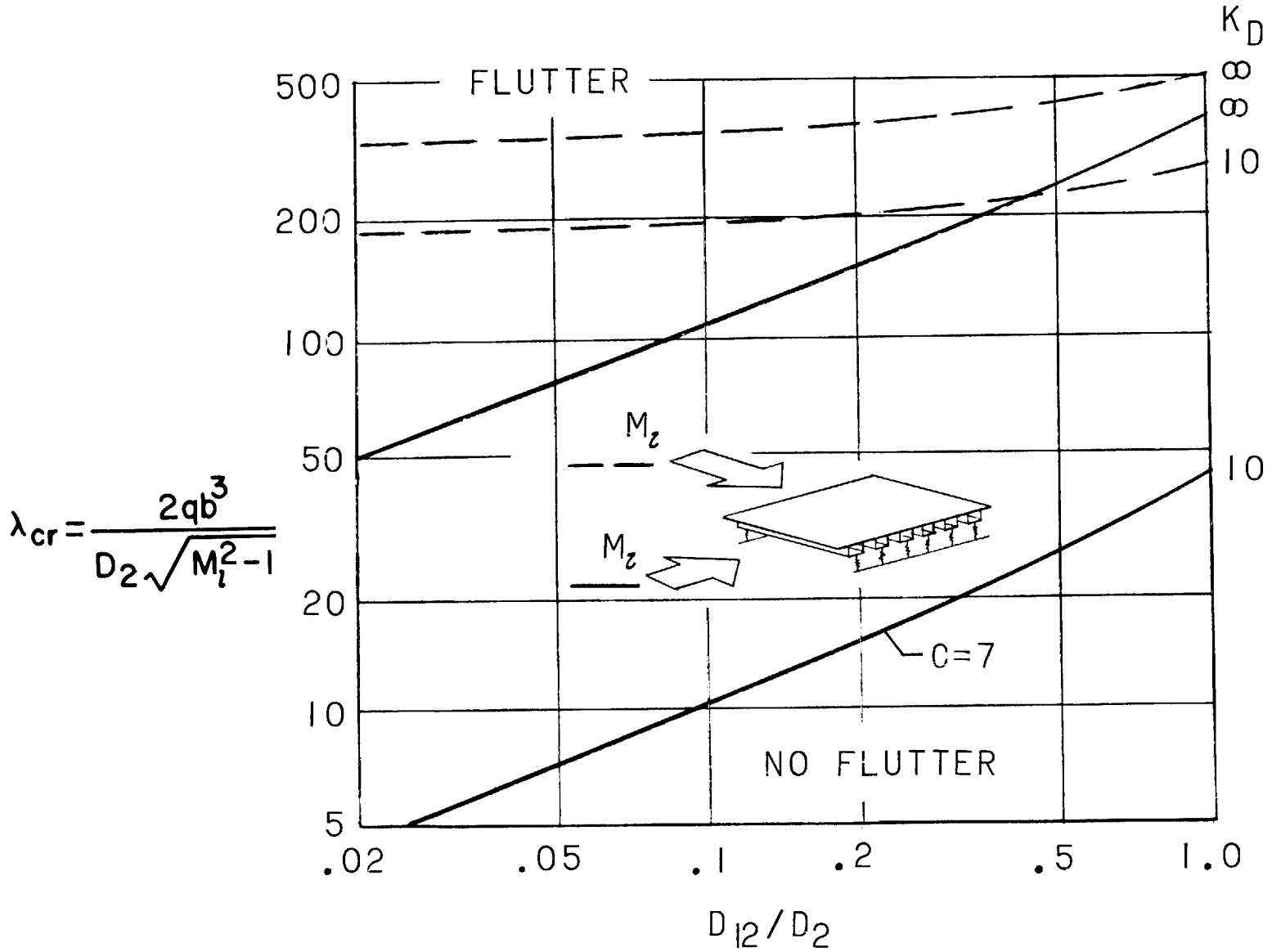

Figure 7.- Effect of panel orientation on flutter boundary. $\frac{a}{b} = 1$.

$$\lambda_{cr} = \frac{2qb^3}{D_2\sqrt{M_l^2 - 1}}$$

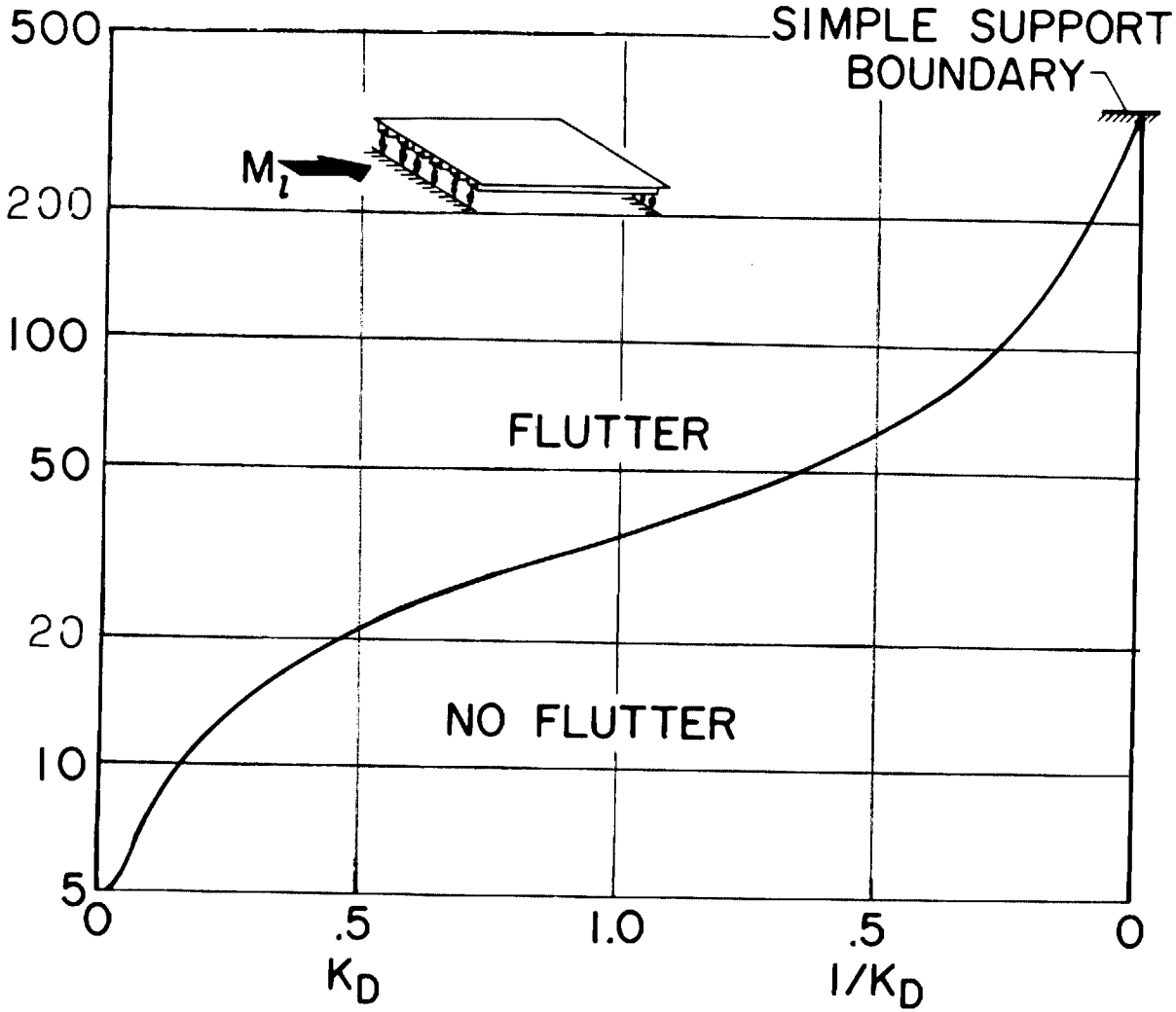

Figure 8.- Minimum flutter boundary for highly orthotropic panels with flow in strong direction.

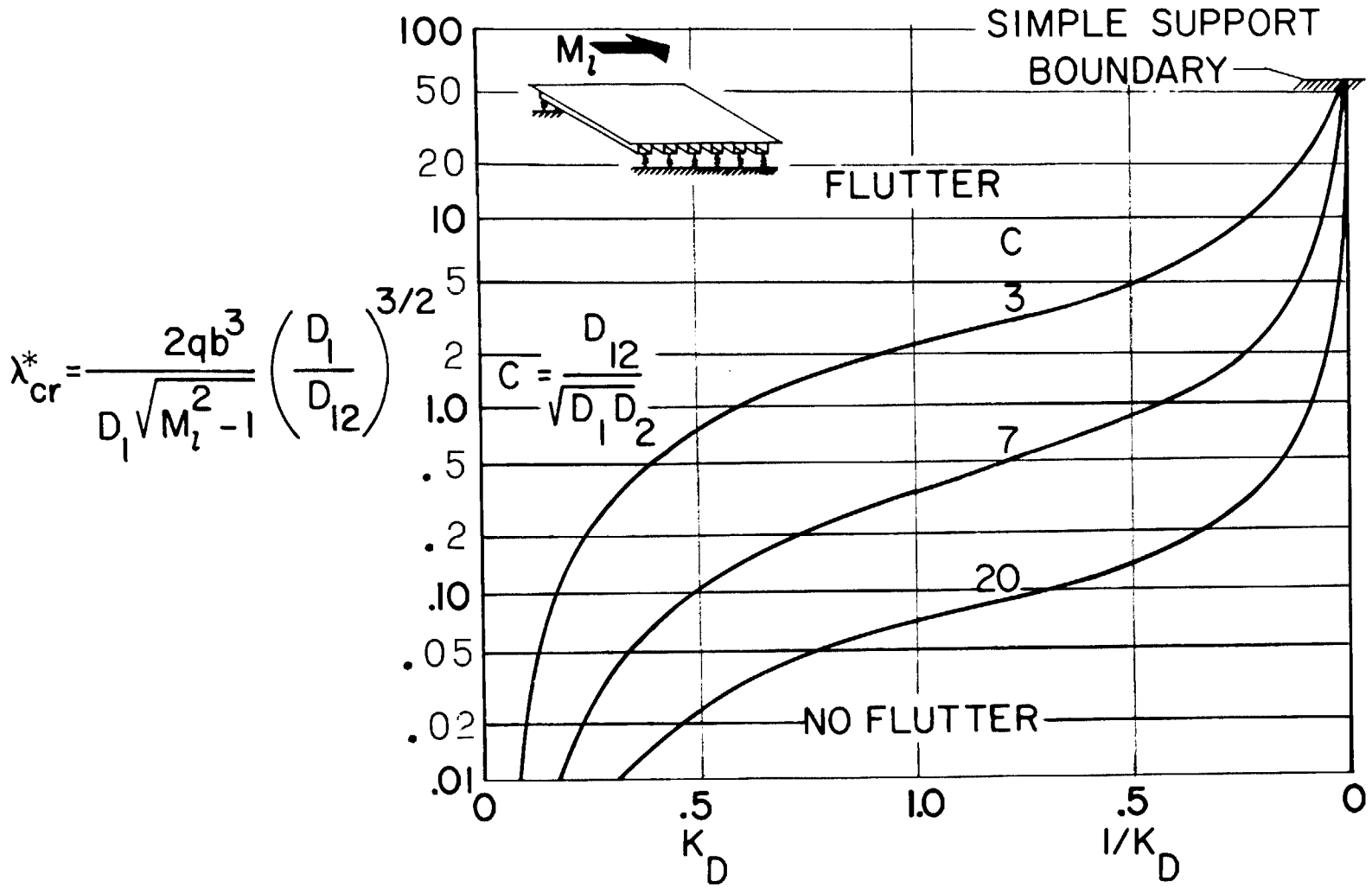

Figure 9.- Minimum flutter boundary for highly orthotropic panels with flow in weak direction.

$$\lambda^*_{cr} = \frac{2qb^3}{D_1\sqrt{M_l^2-1}}\left(\frac{D_1}{D_{12}}\right)^{3/2}$$

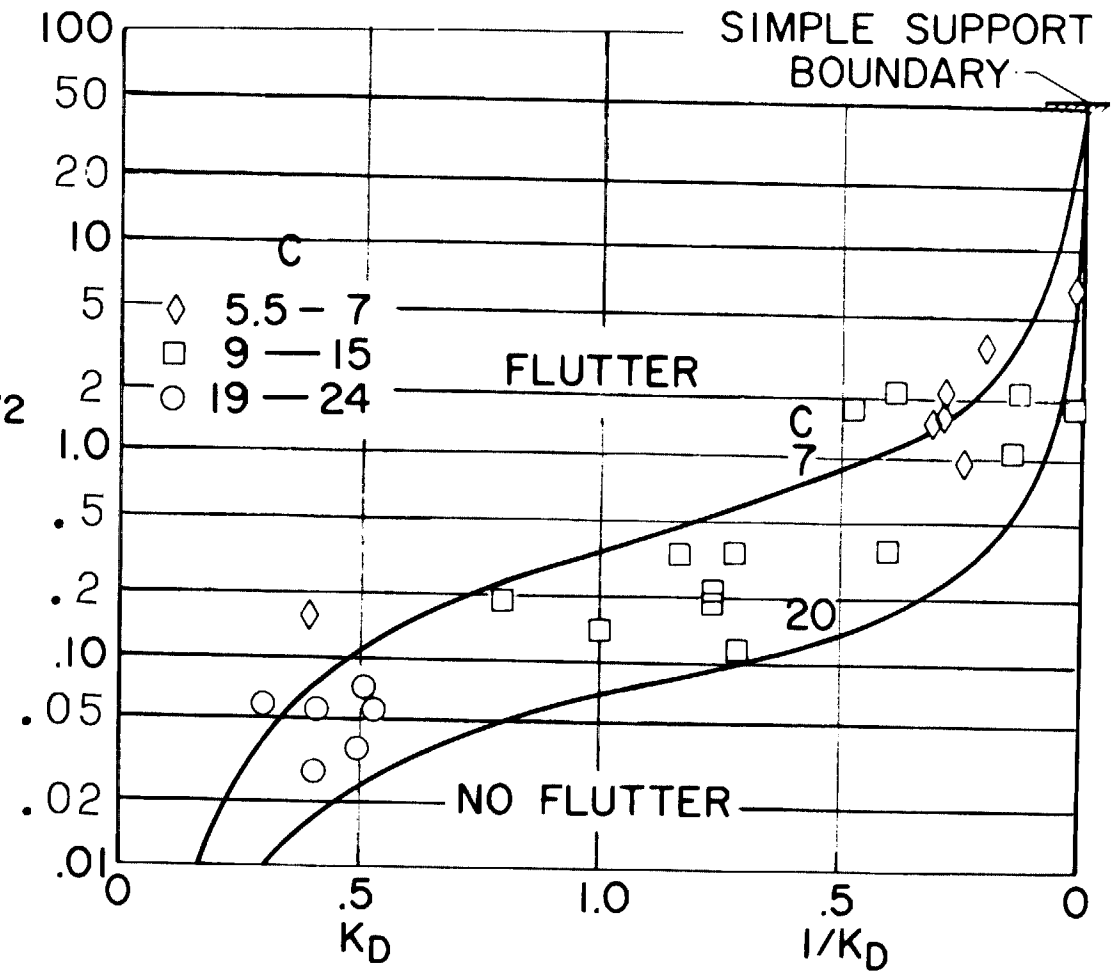

Figure 10.- Comparison of theory and flutter data for orthotropic panels.

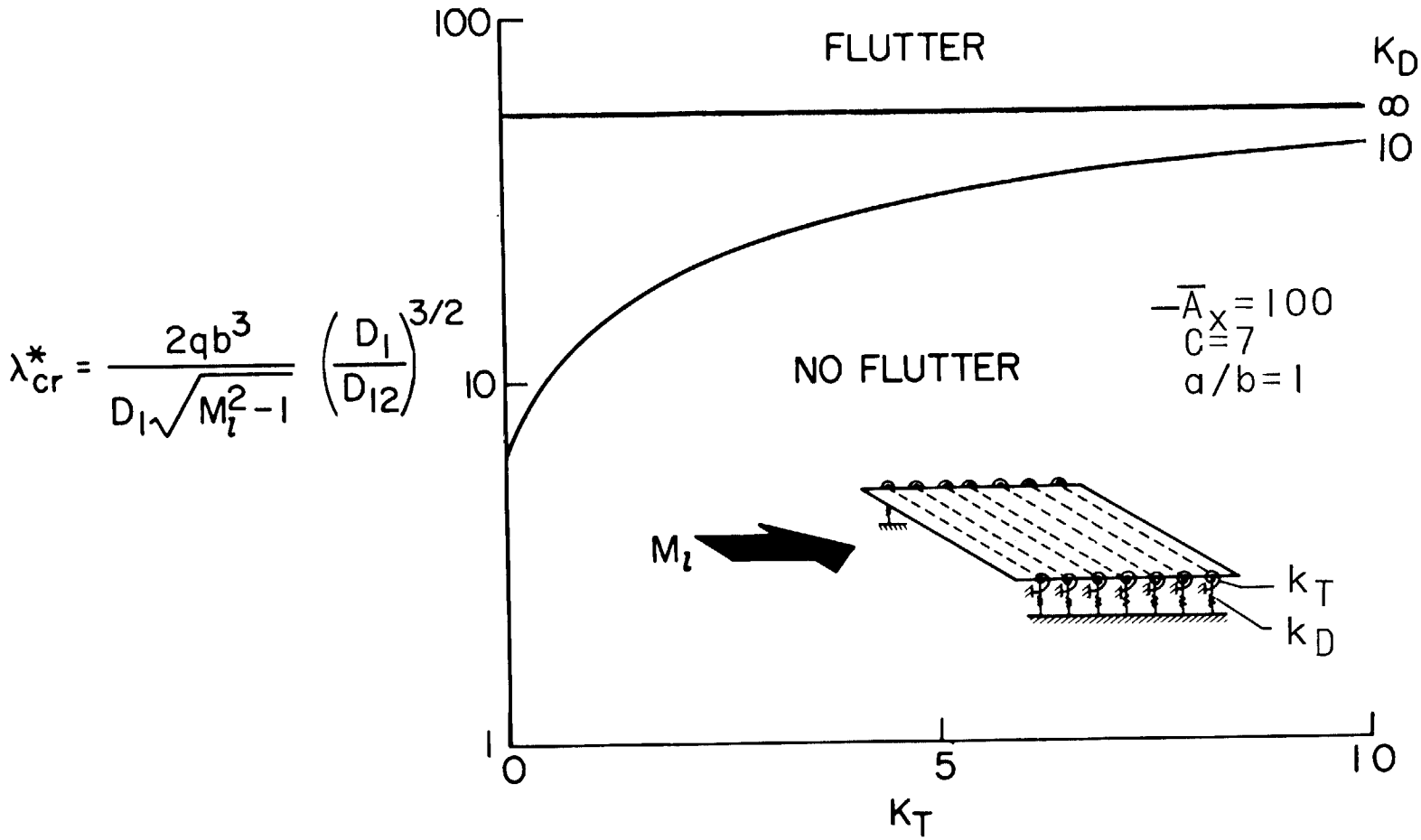

Figure 11.- Effect of edge torsional stiffness.

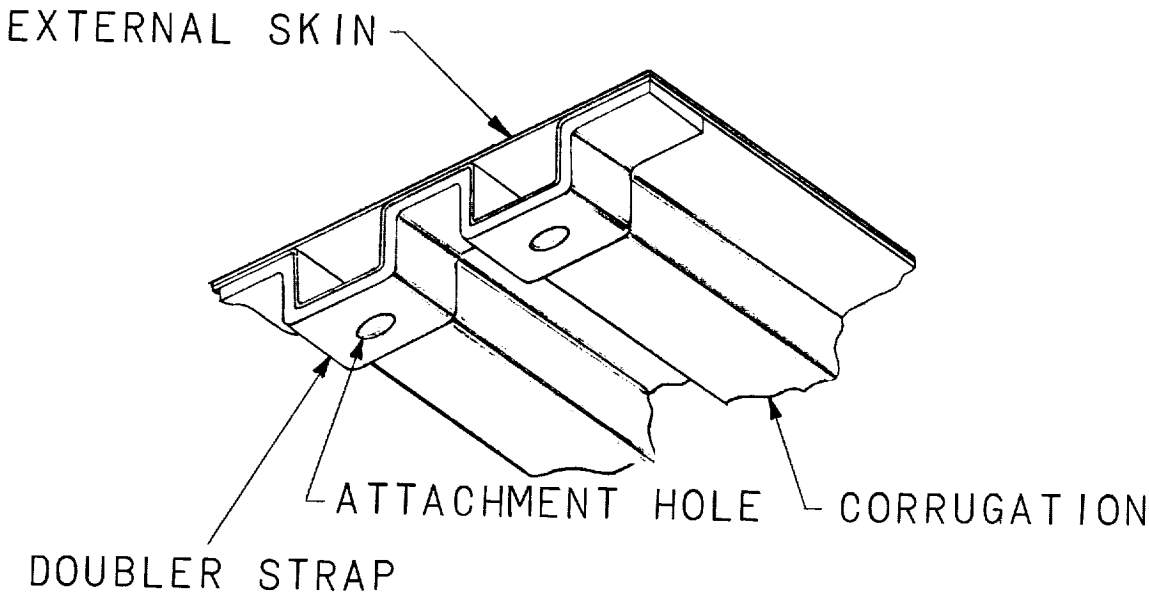

(a) Torsionally stiffened edge.

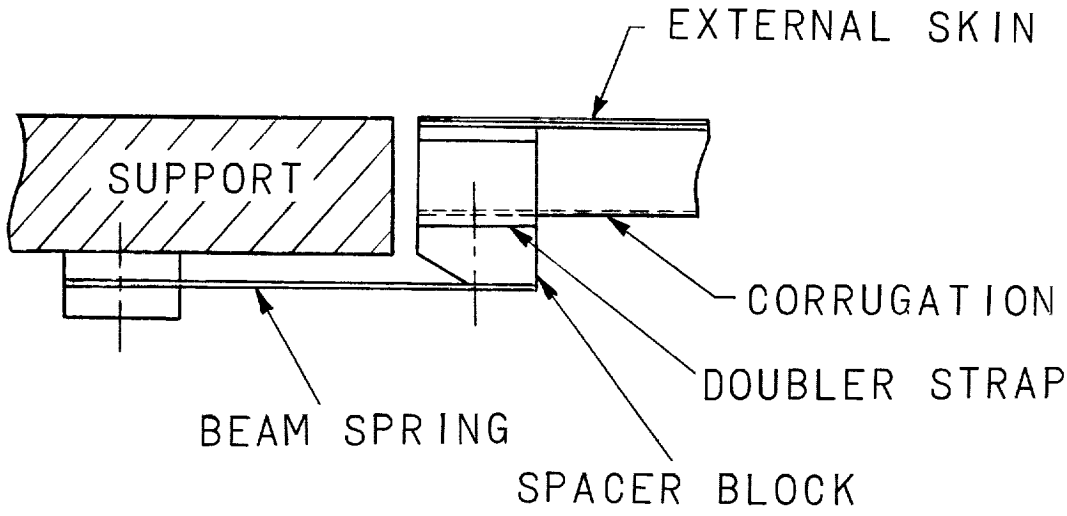

(b) Beam support details.

Figure 12.- Beam-supported corrugation-stiffened panel with torsionally stiffened edge.

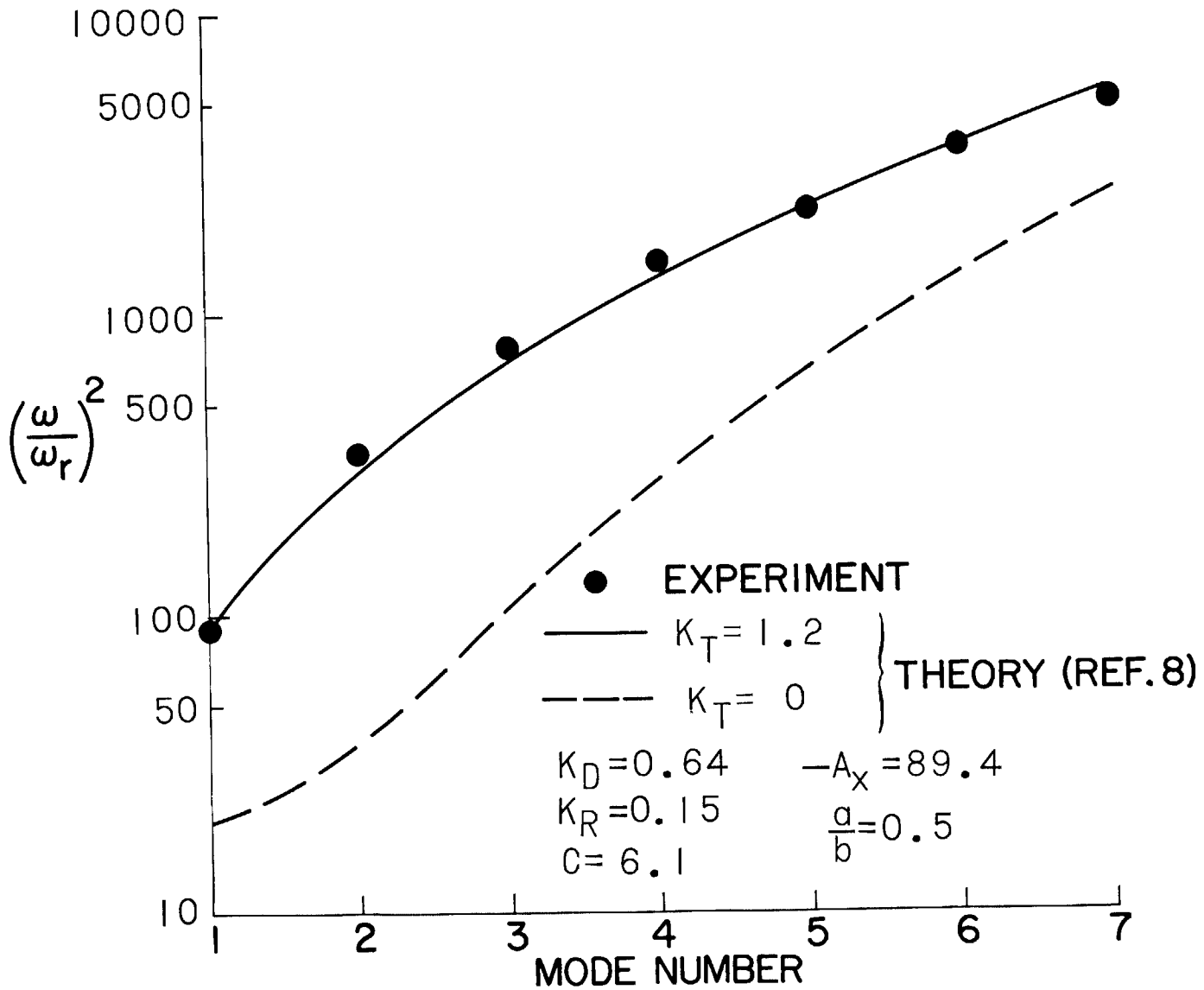

Figure 13.- Comparison of experimental and theoretical natural frequencies.

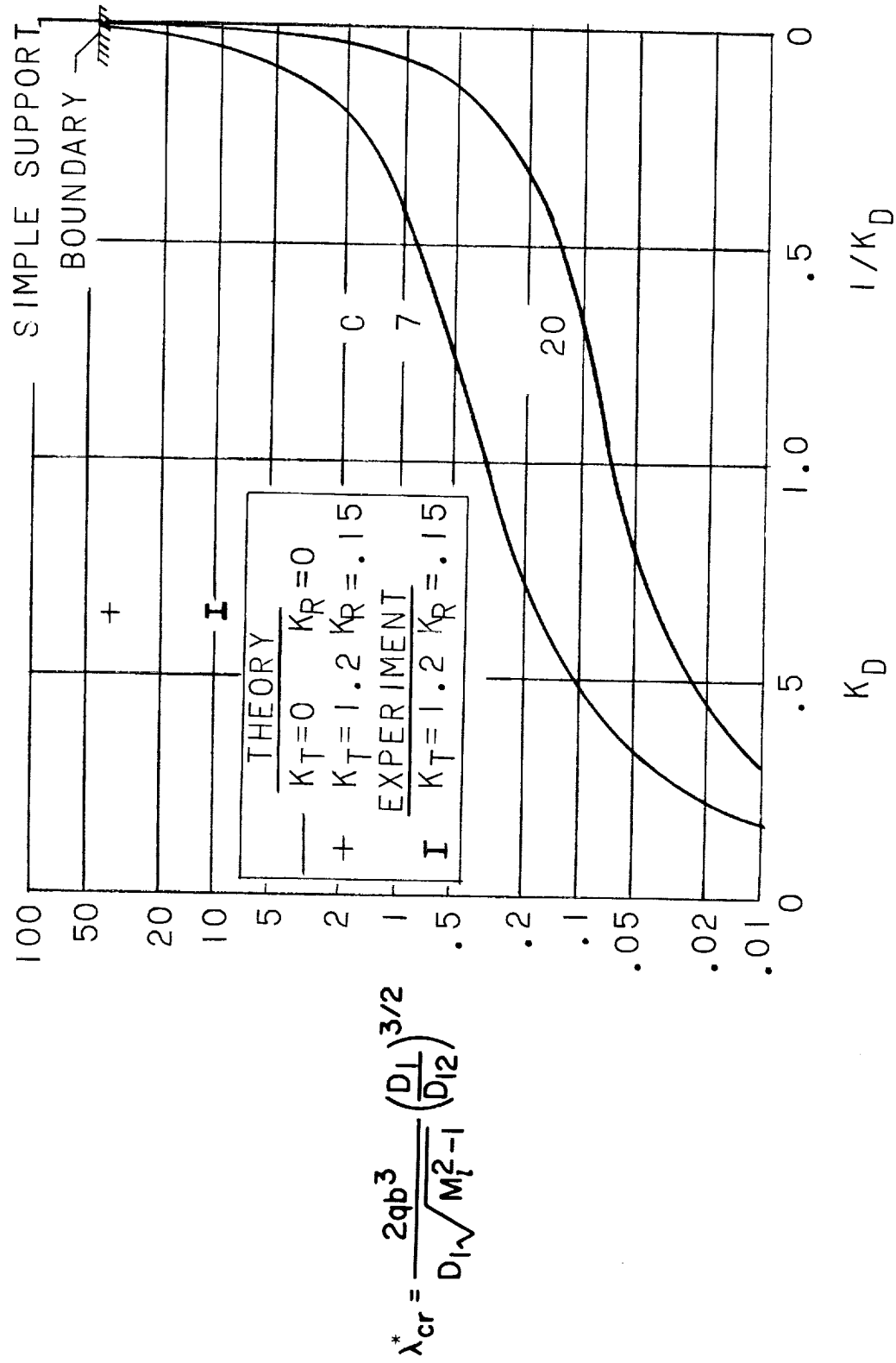

Figure 14.- Comparison of theory and experiment for flutter of torsional restrained panel. C = 6.1.

NASA-Langley, 1969 —— 32 L-6106